New Phytologist

New Phytologist Supporting Information

Article title: **Integration of cell differentiation and initiation of monoterpenoid indole alkaloid metabolism in *Catharanthus roseus* seed germination**

Authors: Mai Uzaki, Tetsuya Mori, Mayuko Sato, Mayumi Wakazaki, Noriko Takeda-Kamiya, Kotaro Yamamoto, Akio Murakami, Delia Ayled Serna Guerrero, Chizuko Shichijo, Miwa Ohnishi, Kimitsune Ishizaki, Hidehiro Fukaki, Sarah E. O'Connor, Kiminori Toyooka, Tetsuro Mimura*, Masami Yokota Hirai*

Article acceptance date: 22 February 2024

The following Supporting Information (8 methods, 21 figures, and 2 tables) is available for this article:

Method S1 Nile blue staining of embryos and leaves

Embryos dissected from 48-HAG seeds and leaves were immersed in 0.1 mg mL^{-1} Nile blue solution (w/v) and dried in a vacuum desiccator (Sanplatec, Osaka, Japan) equipped with a pump (WP6210060, Merck Millipore, Burlington, MA, USA) for 1 h and immersed for 2 days. Leaf sections were prepared using a plant microtome (MTH-1, Nippon Medical and Chemical Instruments, Osaka, Japan).

Methods S2 Fluorescence measurement

In situ fluorescence emission spectra of laticifers in intact hypocotyls of embryos dissected from seeds 48 h after germination (HAG) and a section of the stem were measured using an epi-fluorescence microscope (BX-50, Olympus, Tokyo, Japan) equipped with a multi-channel photodiode detector (PMA-11, Hamamatsu Photonics, Shizuoka, Japan). Excitation light (340–390 nm) was supplied by a 100-W mercury lamp and ultraviolet (UV) light filter unit (U-FUW, Olympus). The fluorescent spectrum of laticifer in leaves was replotted from data provided in Uzaki et al. (2022).

Method S3 Compound analysis using a liquid chromatography (LC)-fluorescence detector

Methanol extracts from leaf, stem, hypocotyl, root, and embryo samples dissected from 48-HAG seeds prepared following the method used for monoterpene indole alkaloid (MIA)/iridoid extraction were analyzed using an ultra-high performance liquid chromatograph (UPLC) (Nexera X2, Shimadzu, Kyoto, Japan) equipped with a fluorescence detector (RF-20A xs, Shimadzu). Chromatographic separation was performed following the same procedure used for MIA measurement. The excitation and emission wavelengths were 405 and 450 nm, respectively.

Method S4 Preparation of semi-thin embryo sections

The samples were fixed with 4% (w/v) formaldehyde, 2% (v/v) glutaraldehyde, and 0.05 M cacodylate buffer overnight at 4°C. The samples were washed six times with 0.05 M cacodylate buffer and then fixed with 1% osmium tetroxide in 0.05 M cacodylate buffer for 1 h. The fixed samples were washed three times with distilled water, dehydrated in a methanol dilution series, and then embedded in EPON 812 resin (TAAB Laboratories, Aldamaston, UK). The resin blocks were sliced using an ultramicrotome (EM-UC7, Leica Microsystems, Wetzlar, Germany) using a

diamond knife (Histo, Diatome, Nidau, Switzerland), and 1-µm-thick sections were mounted on glass slides. Each slide was stained with 0.05% (w/v) toluidine blue and observed with an upright microscope (BX51M, Olympus) to determine which cells to observe in detail through field emission scanning electron microscopy (FE-SEM.)

Method S5 Observation of resin-embedded sections by field emission scanning electron microscope (FE-SEM)

Toluidine blue-stained sections prepared as described above were stained with a 0.4% (w/v) uranyl acetate solution for 12 min, followed by a lead citrate solution for 3 min, and then dried and coated with osmium for 6 s using an osmium coater (HPC-1SW, Vacuum Device, Ibaraki, Japan). Observations and imaging were performed using FE-SEM (SU-8220, Hitachi High Tech, Tokyo, Japan) equipped with a highly sensitive backscatter-electron detector (YAG-BSE; accelerating voltage, 5 kV).

Method S6 RNA extraction and transcriptome analysis

Fifty embryos were collected as a single sample. Frozen samples were ground to a fine powder using a bead crusher (MB601(S) MultiBead Shocker, Yasui Kikai, Osaka, Japan) and total RNA was extracted from the embryos using ISOSPIN Plant RNA (Nippon Gene, Tokyo, Japan) with Assist Buffer for ISOSPIN Plant RNA (Nippon Gene) according to the manufacturer's instructions. Extracted RNA was sequenced using a DNA nanoball sequencing (DNBseq) platform at Azenta Japan (Tokyo, Japan) in 150 bp paired-end mode; more than 6 Gb of raw data (40 million raw reads) per sample was generated. Three biological replicates were performed.

Raw data were processed and quality filtered using trimmomatic v0.38 (Bolger, Lohse and Usadel 2014). Preprocessed reads were mapped to the *Catharanthus roseus* genome deposited in the National Center for Biotechnology Information (NCBI) under accession number PRJNA841429 (Sun et al. 2022) using STAR v2.7.8 (Dobin et al. 2013). Gene raw counts, transcripts per million (TPM), and fragments per kilobase of transcripts per million mapped reads (FPKM) were scored using RSEM v1.3.3 (Li and Dewey 2011). Further analysis was conducted with R v3.6.3 (R Core Team 2020). The data were shaped using the *tidyverse* (Wickham et al. 2019), *dplyr* (Wickham et al. 2021), *stringr* (Wickman 2022), and *Hmisc* (Harrell and Dupont 2021) packages in R. Gene expression was expressed as bar graphs created using the *ggplot2*

(Wickham 2016) and *ggprism* (Dawson 2021) packages in R. Z-scores related to gene expression were calculated and hierarchical clustering analysis and heat mapping were conducted using the *gplots* (Warnes et al. 2020) and *genefilter* (Gentleman et al. 2019) packages in R.

Method S7 Alkaloid staining of section of the leaf and 48-HAG embryos with Dragendorff reagent

Leaves or embryos dissected from 48-HAG seeds were sectioned using a plant microtome (MTH-1, Nippon Medical and Chemical Instruments). After observing the section with a fluorescence microscope (BX53, Olympus), Dragendorff's reagent diluted 1:50 was added to the section for 5 min, and the section was observed.

Methods S8 Non-targeted metabolomic LC–tandem mass spectrometry (MS/MS) analysis

Non-targeted LC-MS/MS analysis of MIAs extracted from embryos was conducted using the Vanquish system (Thermo Fisher Scientific, Massachusetts, USA) system coupled to a Q-Exactive Plus (Thermo Fisher Scientific) orbitrap mass spectrometer. Chromatographic separation was performed using a C18 column (Kinetex XB-C18; particle size, 2.6 μm; pore size, 100 Å; 100 mm × 2.1 mm; Phenomenex, California, USA). The mobile phase consisted of (A) 0.1% (v/v) formic acid and (B) 0.1% (v/v) formic acid in acetonitrile. The elution program was optimized as follows: 10–30% B (0–6 min), 90% B (6–7.5 min), 100% B (7.5–8 min), 10% B (8–10 min). The column was maintained at 40°C throughout the analysis. The injection volume was 1 μL and the flow rate was 0.6 mL min^{-1}. The MS was performed following heated electrospray ionization (HESI) with the source in positive ion detection mode and the MS spectrometer was used in full-scan data-dependent MS/MS mode. At least five biological replicates were performed. The data were analyzed using MS-DIAL v4.90 (Tsugawa et al. 2015).

Fig. S1 Sample preparation procedure for imaging mass spectrometry (IMS) analysis.
Frozen sections were prepared using a cryostat and attached to copper tape on an indium tin oxide glass slide, and freeze-dried. Then, α-cyano-4-hydroxycinnamic acid (CHCA) matrix was applied to the freeze-dried taped sections. Further details are provided in Materials and Methods.

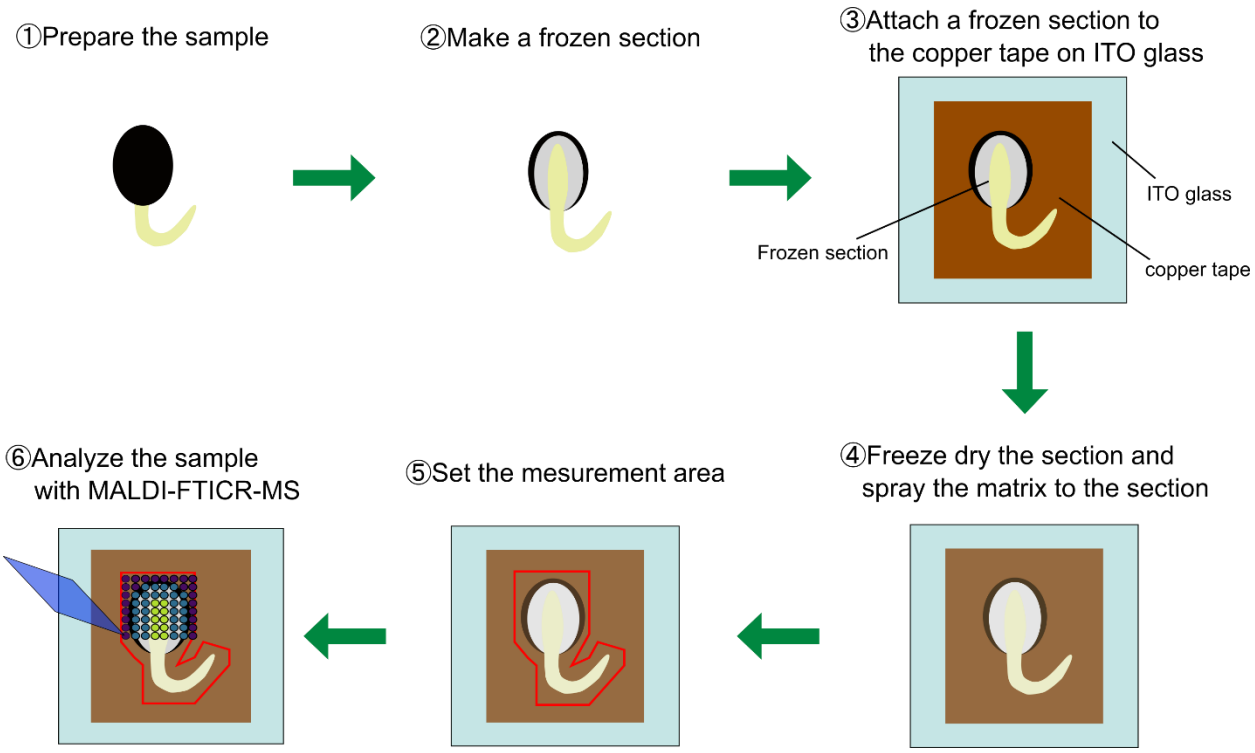

Fig. S2 Changes in the germination rate of *C. roseus* seeds after the start of imbibition.

The germination rate was calculated from the number of germinated seeds in a dish initially containing 60 seeds. n = 5.

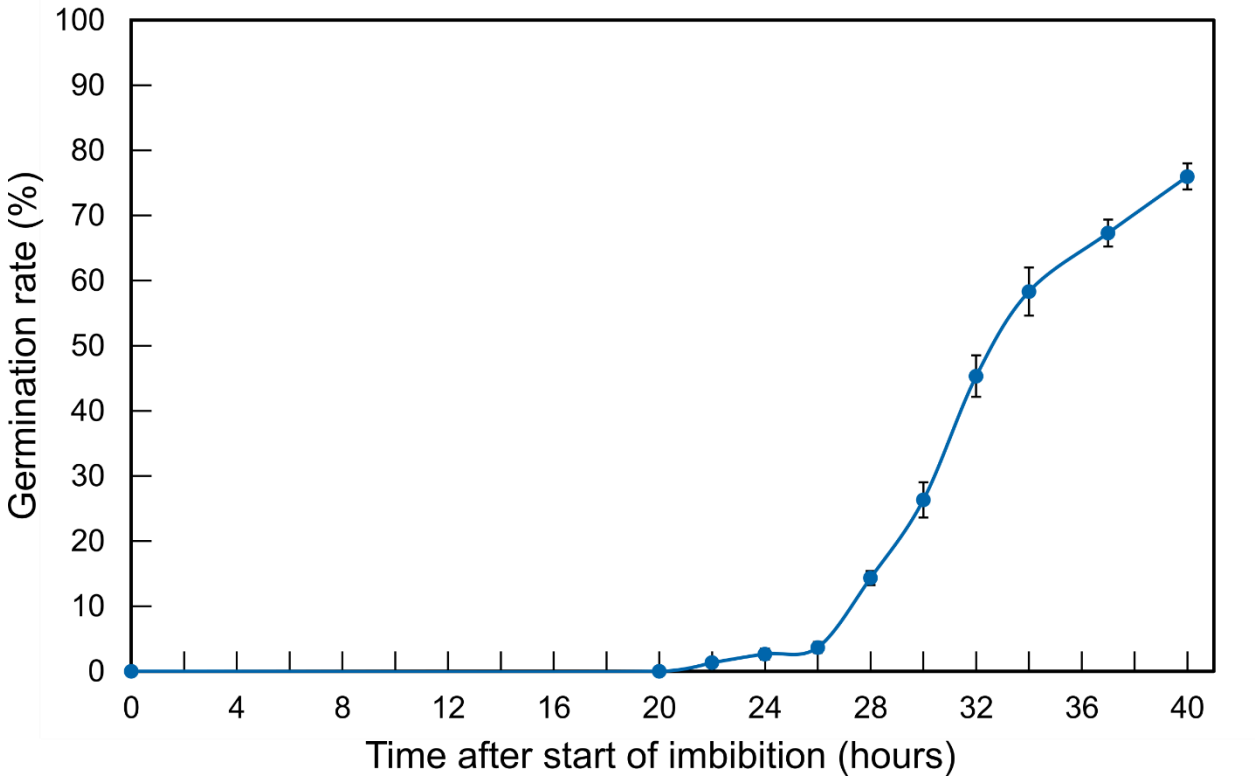

Fig. S3 Microphotographs of sections of embryos dissected from 48 h after germination (HAG) seeds.

(**a**, **d**) Section of embryos of 48-HAG seeds. (**b**, **e**) Fluorescence microscopic images of the sections as shown in (**a**) or (**d**). (**c**, **f**) Magnification of the boxed area shown in (**b**) or (**e**). The yellow arrows in (**b**) and (**c**) indicate the laticifers, while orange arrows in (**e**) and (**f**) indicate xylem. Scale bars are 200 μm.

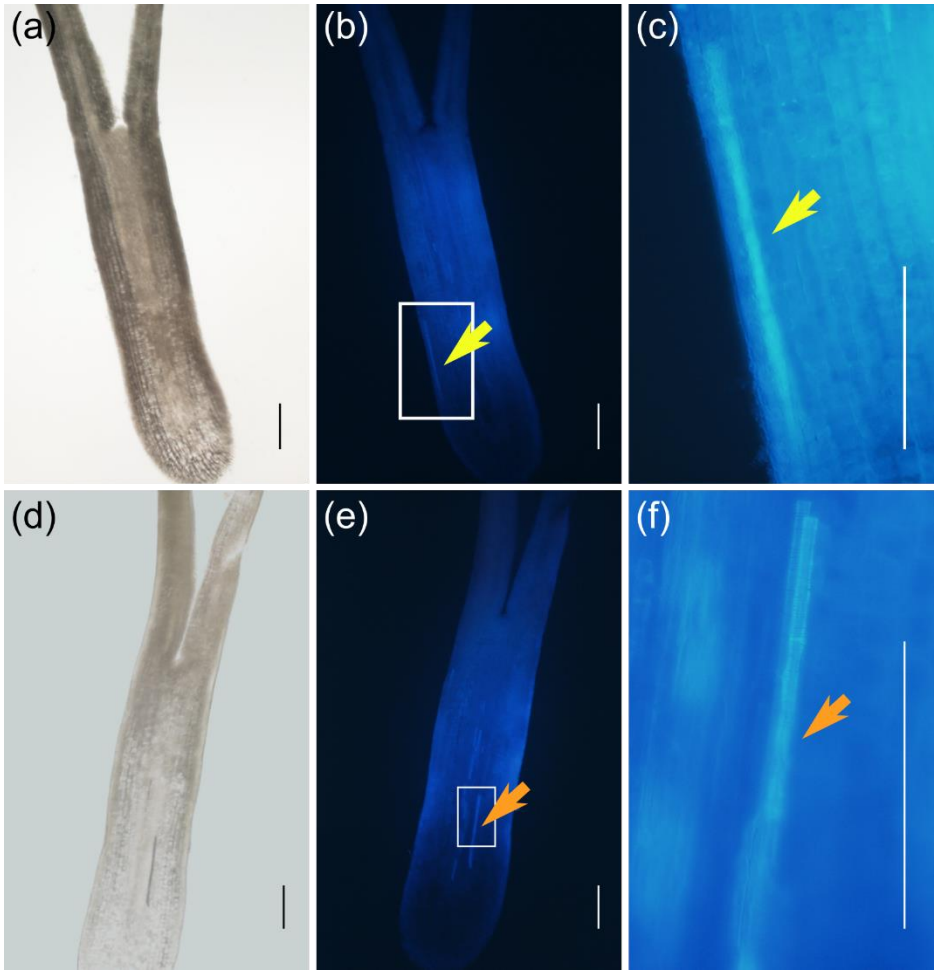

Fig. S4 Nile blue staining of leaves and embryos of 48-HAG seeds.

(**a**, **b**) Stereomicroscopic images of a leaf before (**a**) before and after (**c**) Nile blue staining. (**b**) Fluorescence microscopic image of the leaf shown in (**a**). (**d**) Upright and (**e**) fluorescence microscopic images of leaf sections. (**f**) Nile blue-stained leaf section. This section is different from those shown in (**d**) and (**e**). (**g**) Nile blue-stained embryos of 48-HAG seeds. (**h**, **i**) Magnified images of the boxed area of in (**g**). Scale bars are (**a**–**c**) 500 μm or (**d**–**i**) 200 μm.

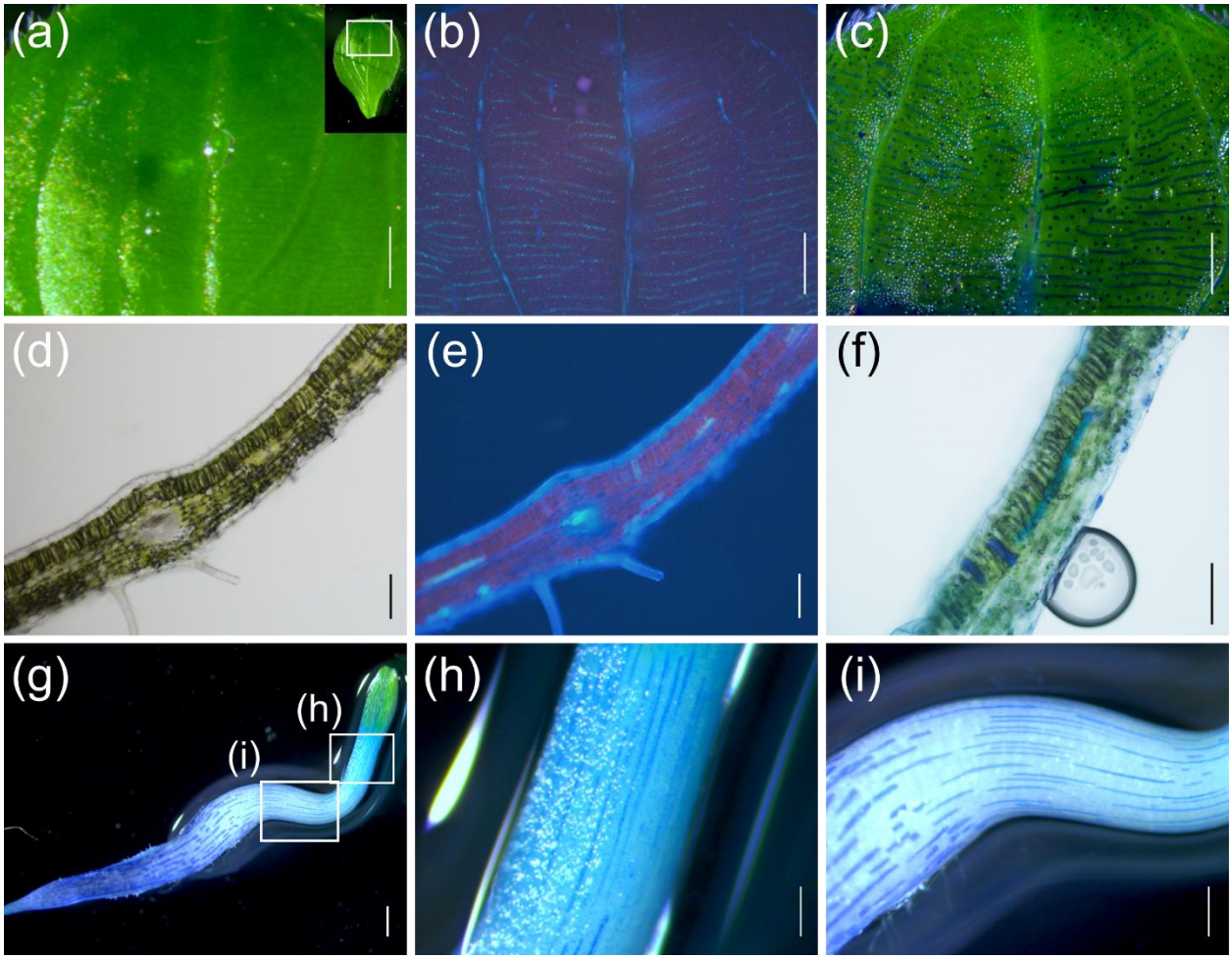

Fig. S5 Comparison of the fluorescence spectra of laticifers.

(**a**) Ultraviolet light-excited fluorescence spectrum of laticifers in the hypocotyl of a 48-HAG embryo (top), leaf (middle), and stem (bottom).

(**b**) Chromatogram of methanol extracts from matured tissues and 48 HAG seeds obtained by ultra-high-performance liquid chromatography (UPLC) with a fluorescence detector.

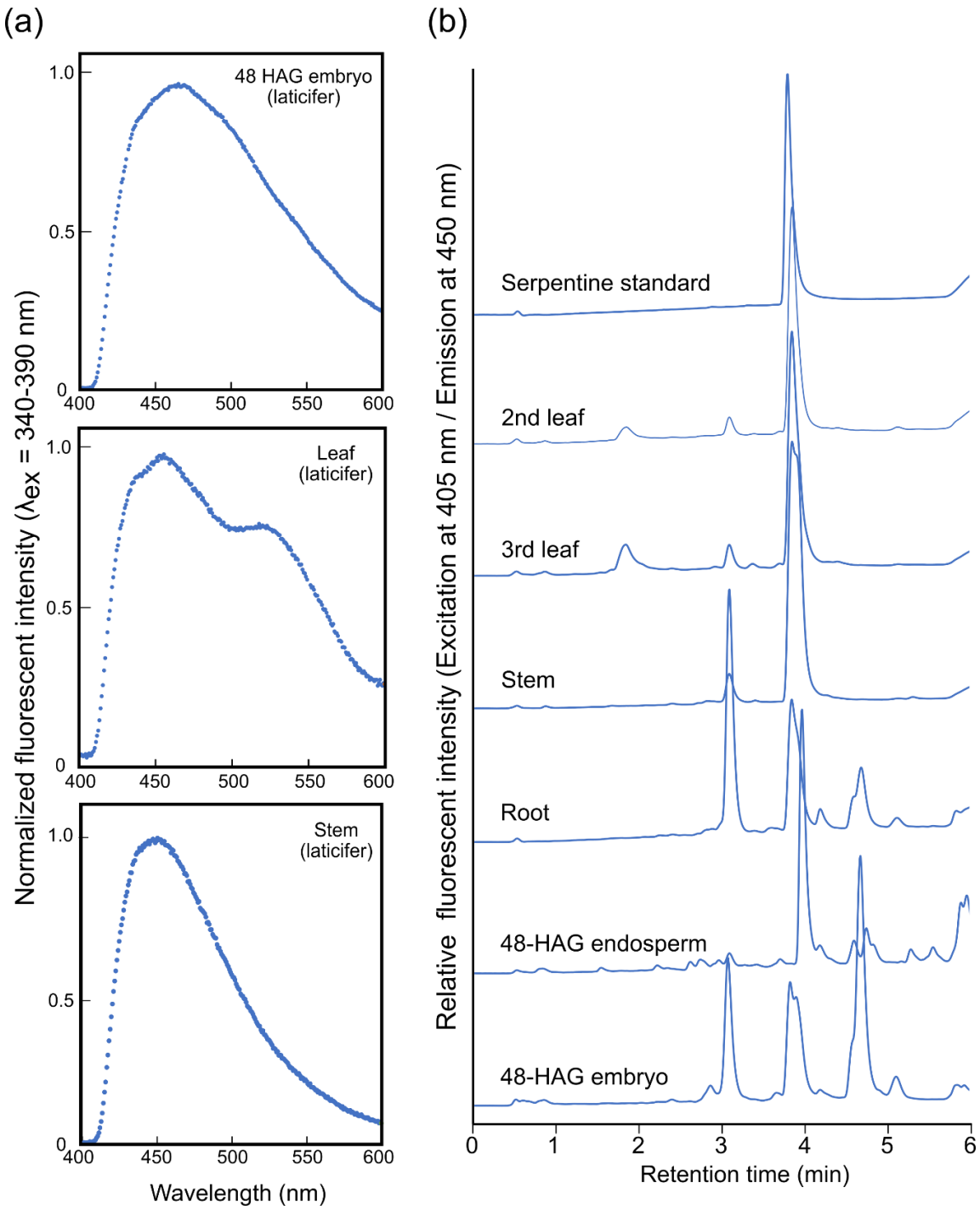

Fig. S6 Microphotographs of semi-thin sections of embryos dissected from immature seeds. Upright microscopic images of laticifers in two embryos dissected from immature seeds. (**b**, **c**, **e**, **f**); Magnified images of the boxed area in (**a**) or (**d**). Laticifers are indicated by red dashed lines. Scale bars are (**a**, **d**) 500 μm, (**b**, **c**, **e**) 50 μm, or (**f**) 200 μm.

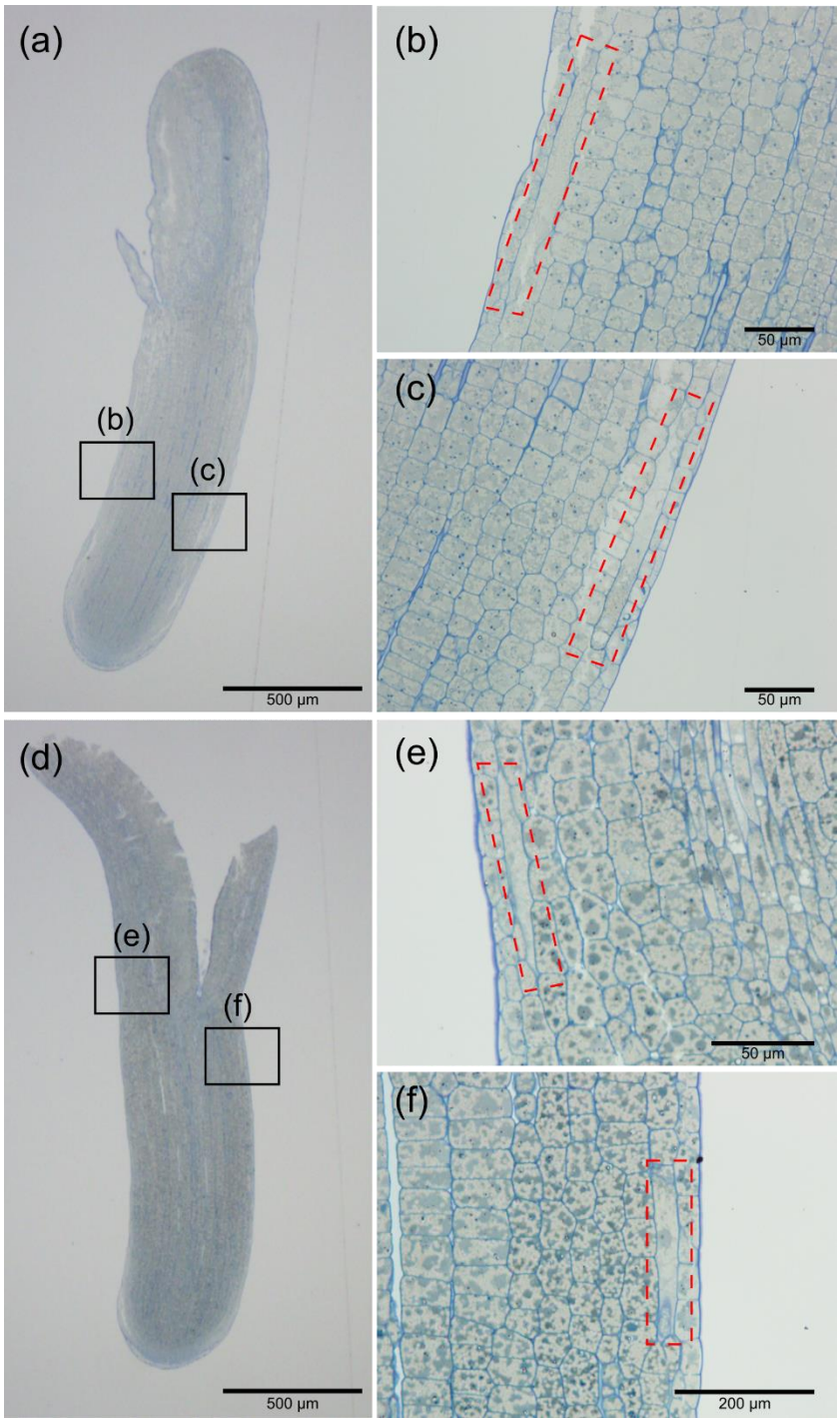

Fig. S7 Microphotographs of semi-thin sections of embryos dissected from germinating seeds. Upright microscopic images of laticifers in (**a**) 0, (**d**) 12, (**g**) 24, and (**j**) 36-HAG embryos. Scale bars are 500 μm. (**b**, **c**, **e**, **f**, **h**, **i**, **k**, **l**) Magnified images of the boxed area in (**a**), (**d**), (**g**), and (**j**). Laticifers are indicated by red dashed line. Scale bars are (**b**, **c**, **e**, **f**, **h**, **i**, **k**) 50 μm or (**l**) 200 μm.

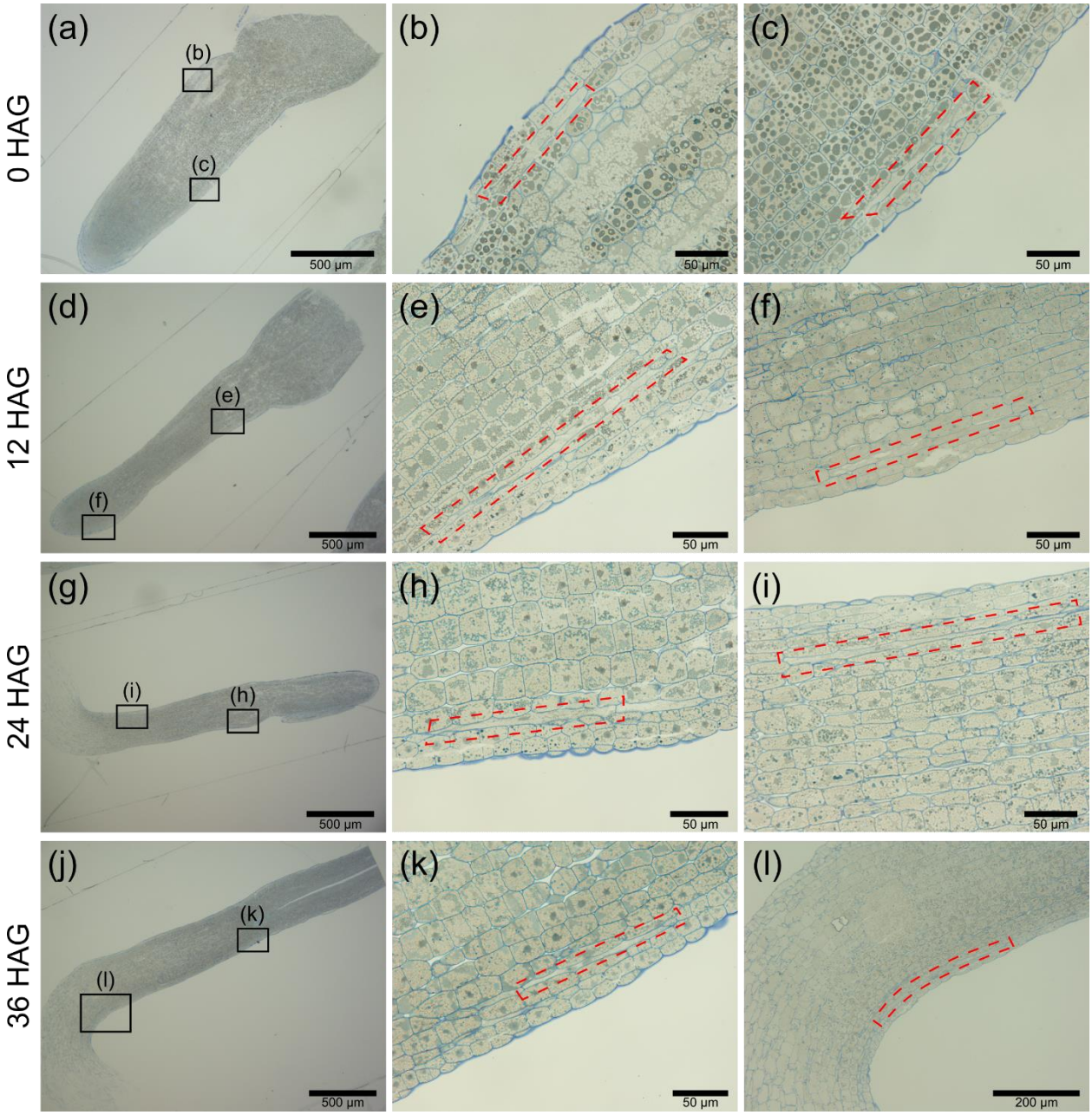

Fig. S8 Electron micrograph images of laticifers in embryos dissected from immature seeds. Field emission scanning electron microscopy (FE-SEM) images of laticifers in embryos dissected from immature seeds. Laticifers are surrounded by yellow dashed lines in (**a**) and (**f**). (**b**, **c**, **d**, **e**, **g**, **h**, **i**, **j**) Magnified images of the boxed area in (**a**) or (**f**). Scale bars are (**a**, **f**) 30 μm, (**b**, **c**, **d**, **e**, **g**, **h**, **i**, **j**) 10 μm. EV, embryonic vacuole; LD, lipid droplet; N, nucleus; PSV, protein storage vacuole.

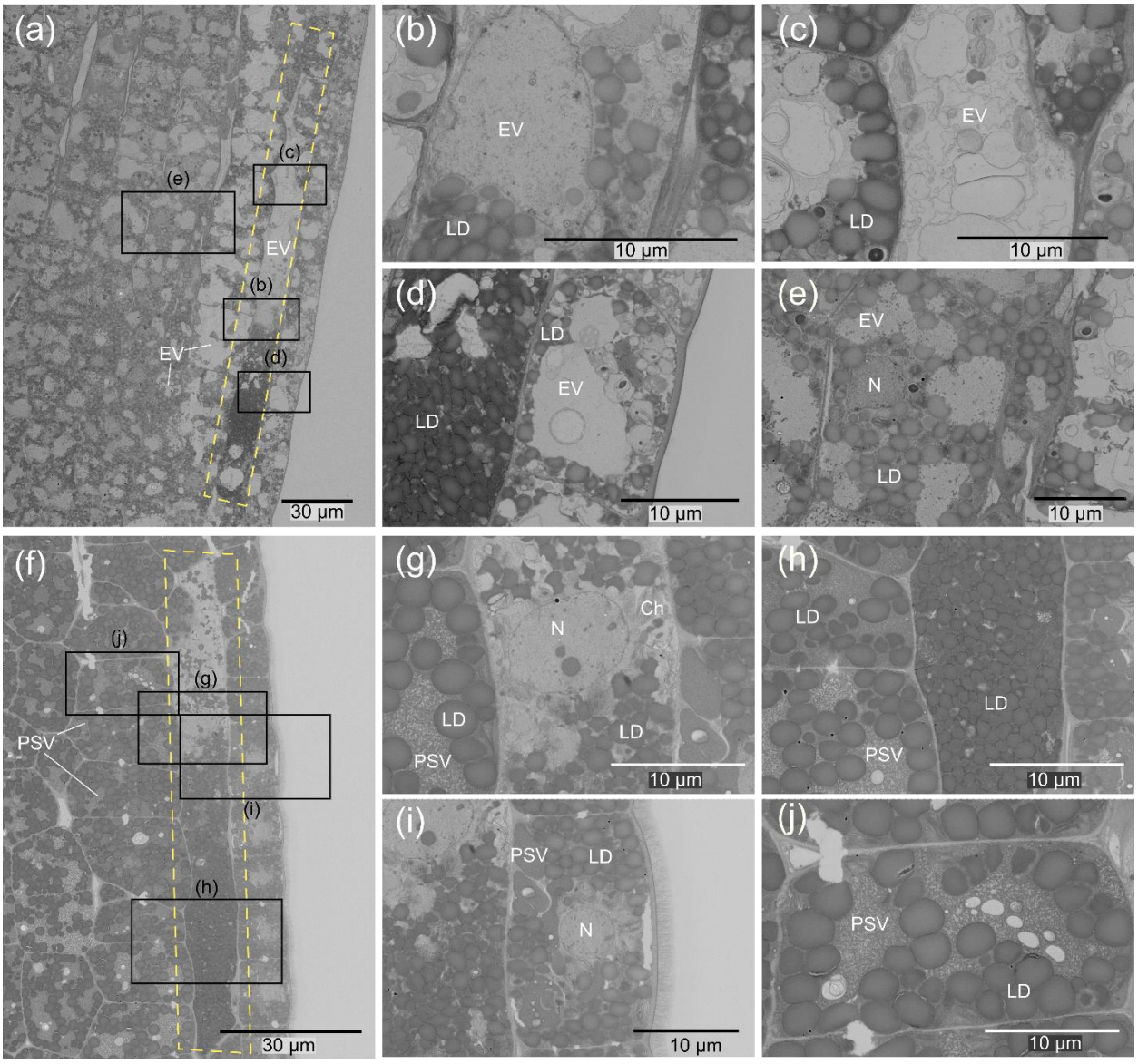

Fig. S9 Electron micrograph images of laticifers in the hypocotyl near the radicle.

FE-SEM image of laticifers in seeds dissected at (**a**) 0, (**d**) 12, (**g**) 24, and (**j**) 36 HAG. Scale bars are 100 μm. Laticifers are surrounded by yellow dashed lines. (**b**, **c**, **e**, **f**, **h**, **i**, **k**, **l**) Magnified images of the boxed area in (**a**), (**d**), (**g**), or (**j**). Scale bars are (**b**, **h**, **i**, **k**, **l**) 10 μm, (**c**, **f**) 5 μm, or (**e**) 20 μm. EV, embryonic vacuole; LD, lipid droplet; LV, lytic vacuole; N, nucleus; P, plastid; PSV, protein storage vacuole.

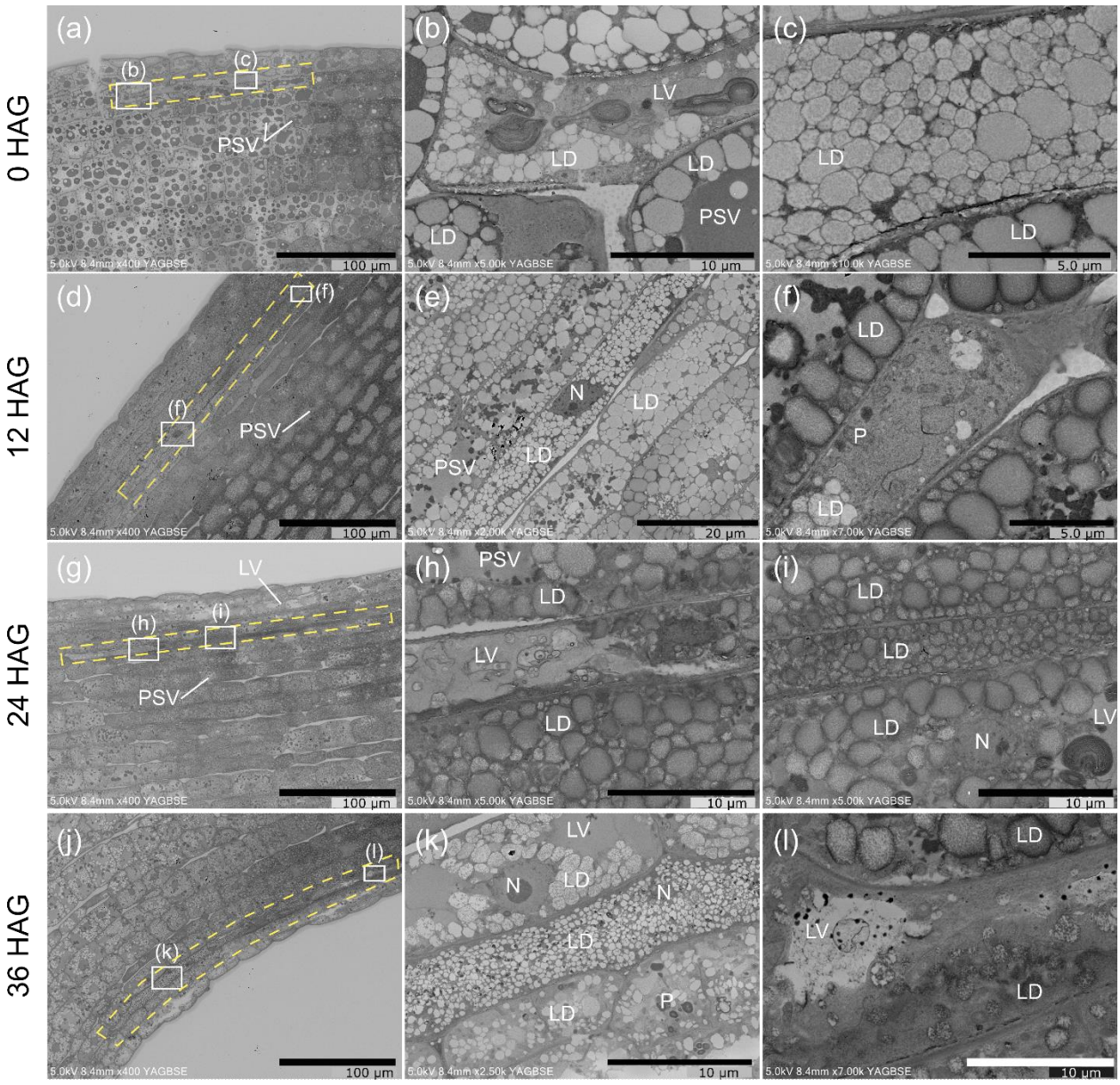

Fig. S10 Electron micrographs of the epidermal and cortical cells around the laticifer in the hypocotyl near the cotyledon.

FE-SEM images of epidermis and cortical cells around laticifers in embryos from seeds dissected at (**a**) 0, (**d**) 12, (**g**) 24, and (**j**) 36 HAG. Laticifers are surrounded by yellow dashed lines. Scale bars are 100 μm. (**b**, **c**, **e**, **f**, **h**, **i**, **k**, **l**) Magnified images of the boxed areas in (**a**), (**d**), (**g**), or (**j**). Scale bars are 10 μm. LD, lipid droplet; LV, lytic vacuole; N nucleus; P, plastid; PSV, protein storage vacuole.

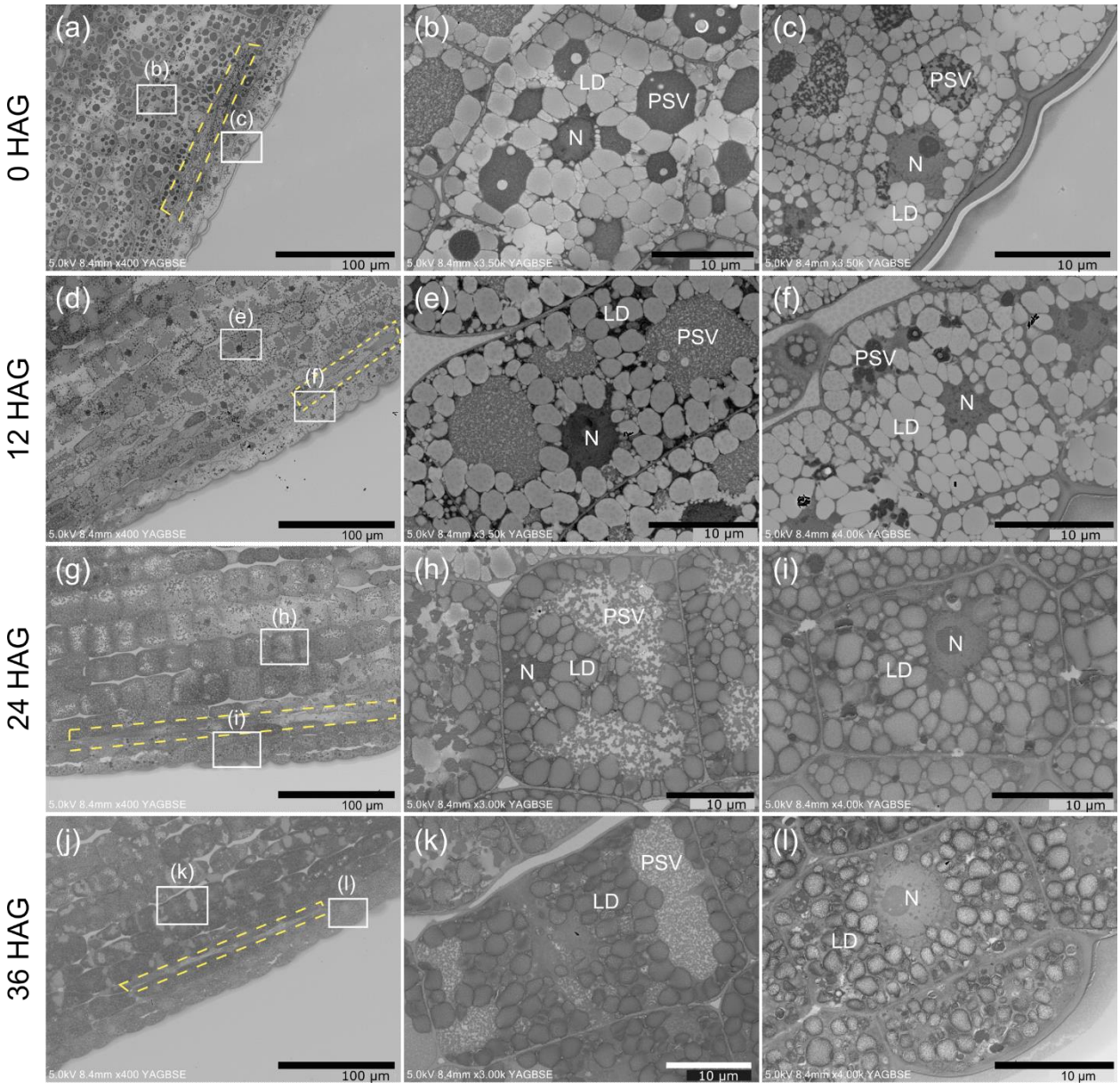

Fig. S11 Electron micrographs of epidermal and cortical cells around the laticifer in the hypocotyl near the radicle.

FE-SEM images of epidermal and cortical cells around laticifer cells in embryos from seeds dissected at (**a**) 0, (**d**) 12, (**g**) 24, and (**j**) 36 HAG. Laticifers are surrounded by yellow dashed lines. Scale bars are 100 μm. (**b**, **c**, **e**, **f**, **h**, **i**, **k**, **l**) Magnified images of the boxed area in (**a**), (**d**), (**g**), or (**j**). Scale bars are (**b**, **c**, **e**, **f**, **i**, **k**, **l**) 10 μm or (**h**) 20 μm. LD, lipid droplet; LV, lytic vacuole; N, nucleus; P, plastid; PSV, protein storage vacuole.

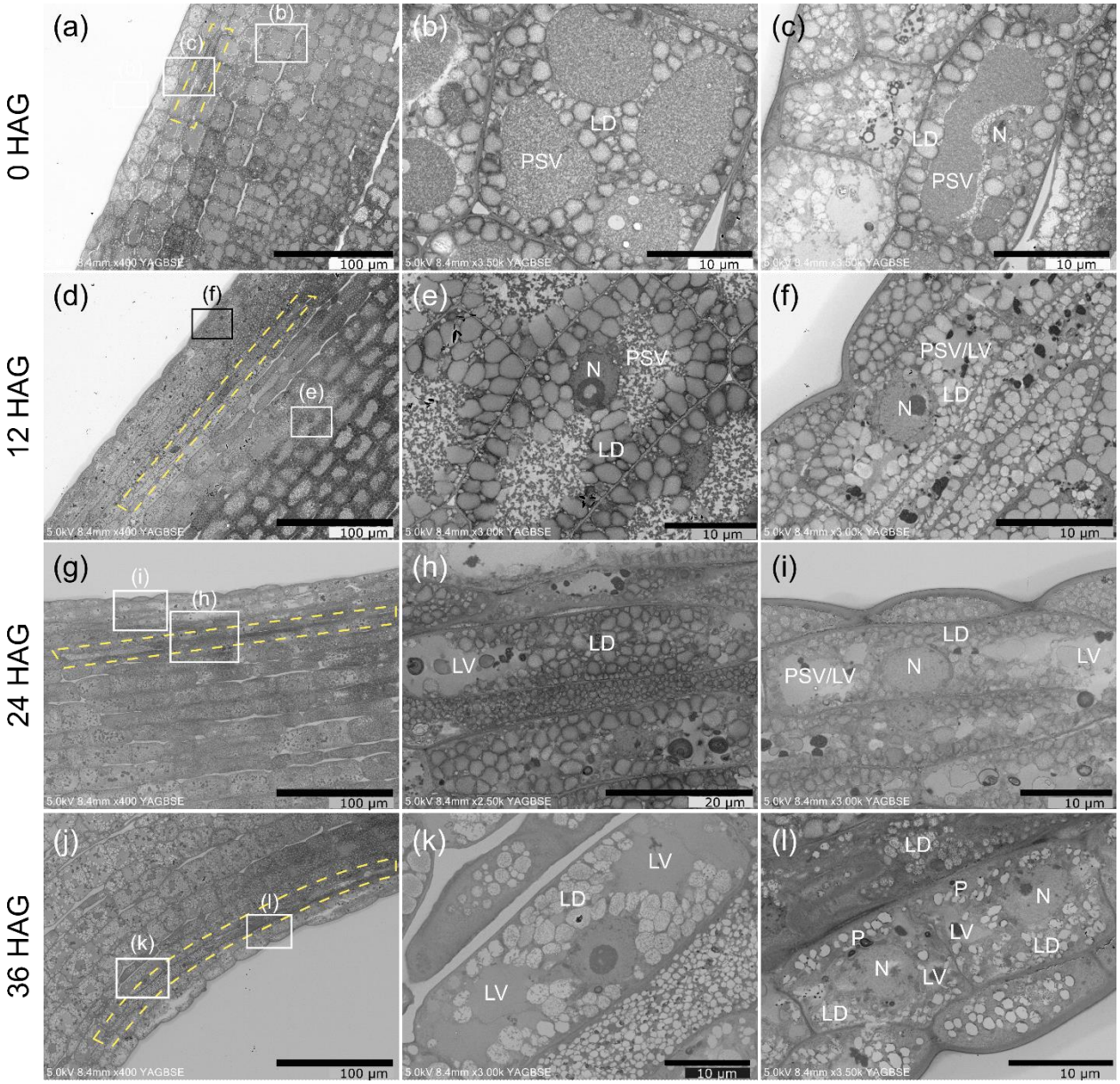

Fig. S12 Electron micrographs of laticifers with two nuclei found in embryos of 12- and 24-HAG seeds.

Electron micrographs of multinucleated laticifers found in embryos of (**a**) 12- and (**d**) 24-HAG seeds. Laticifers are surrounded by yellow dashed lines. (**b**, **c**, **e**, **f**) Magnified images of the boxed area including nucleus in (**a**) or (**d**). Scale bars are (**a**) 100 μm or (**b**, **c**, **e**, **f**) 10 μm.

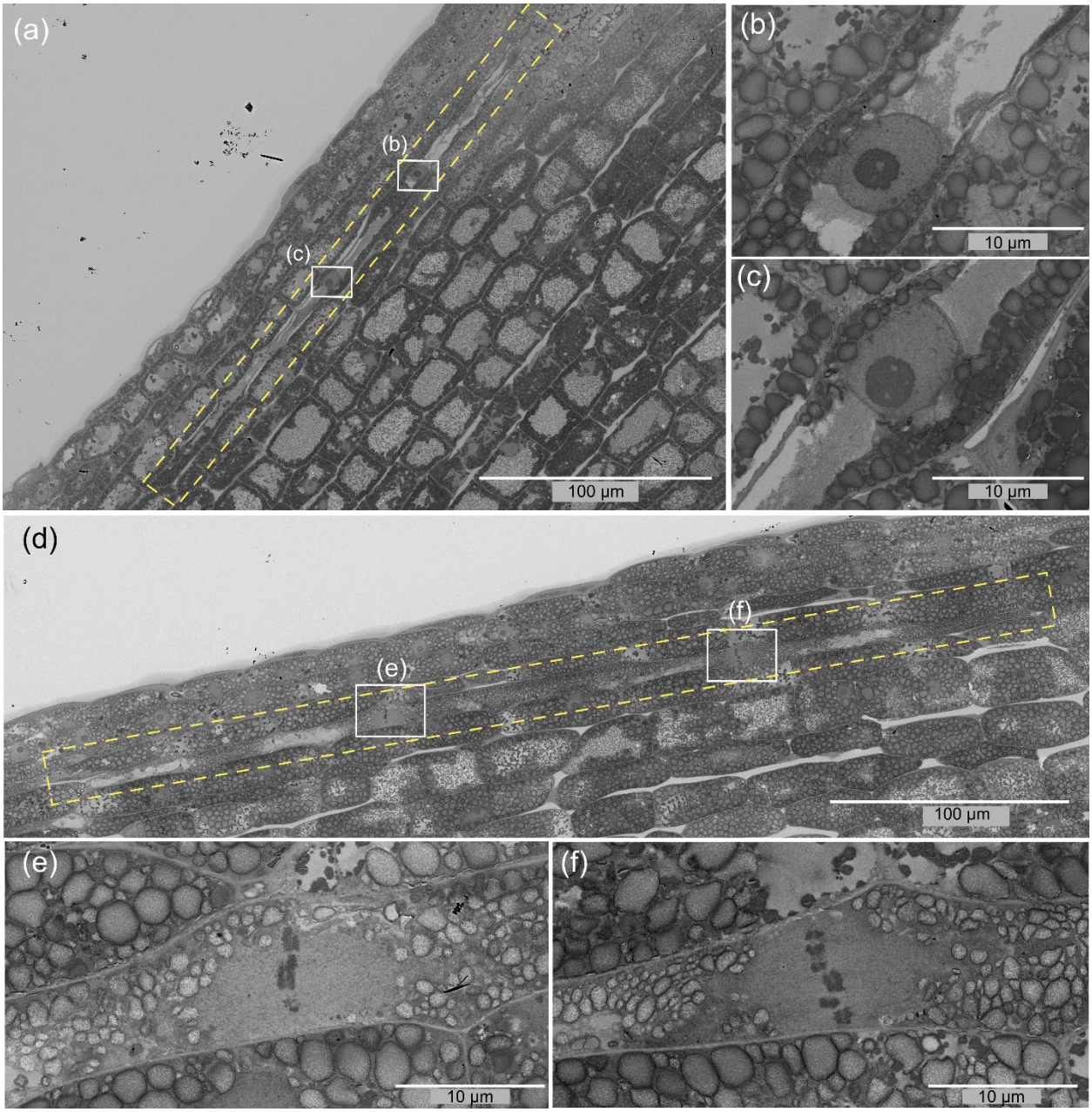

Fig. S13 Electron micrographs of multinucleated laticifers found in embryos of 36-HAG seeds.

Electron micrographs of laticifers found in embryos of 36-HAG seeds, having (**a**) two or (**d**) six nuclei. Elongated laticifer is surrounded by yellow dashed lines. (**b**, **c**, **e**, **f**, **g**, **h**, **i**) Magnified images of the boxed area including nucleus in (**a**) or (**d**). Scale bars are (**a**) 100 μm, (**f**, **g**, **h**, **i**) 10 μm, (**b**, **c**, **j)** 5.0 μm, or (**e**) 4.0 μm.

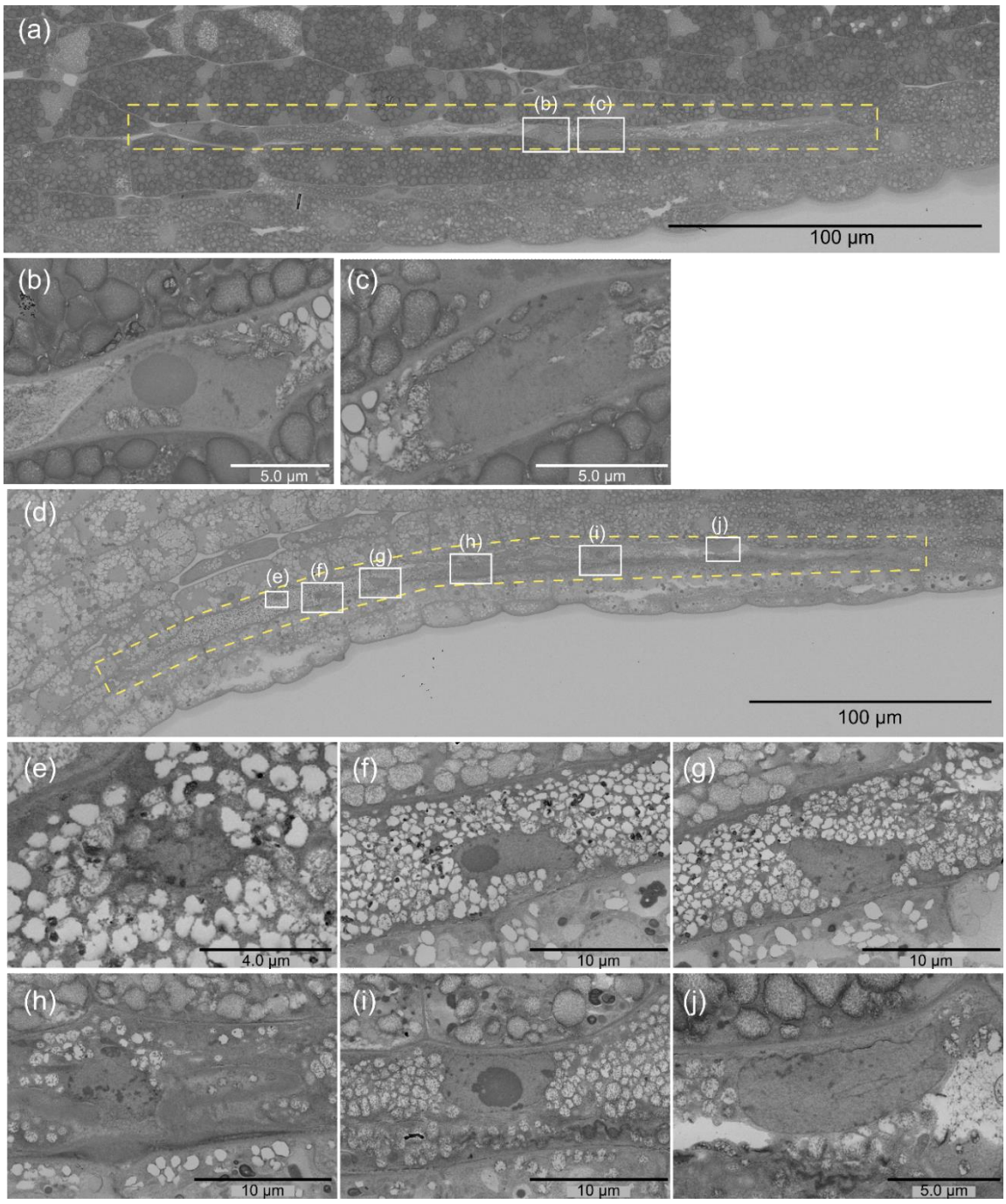

Fig. S14 Monoterpene indole alkaloid (MIA) content of mature tissues.

Bar graphs show average MIA (tryptamine, strictosidine, tabersonine, diacetyl vindoline, vindoline, catharanthine, ajmalicine, and serpentine) contents (nmol/mg) of leaves, stems, hypocotyls, and roots (n = 5). Each plot represents one sample. Bis-indole alkaloids such as 3,4-anhydrovinblastine were below the limit of quantitation in all samples. n.d., not detected.

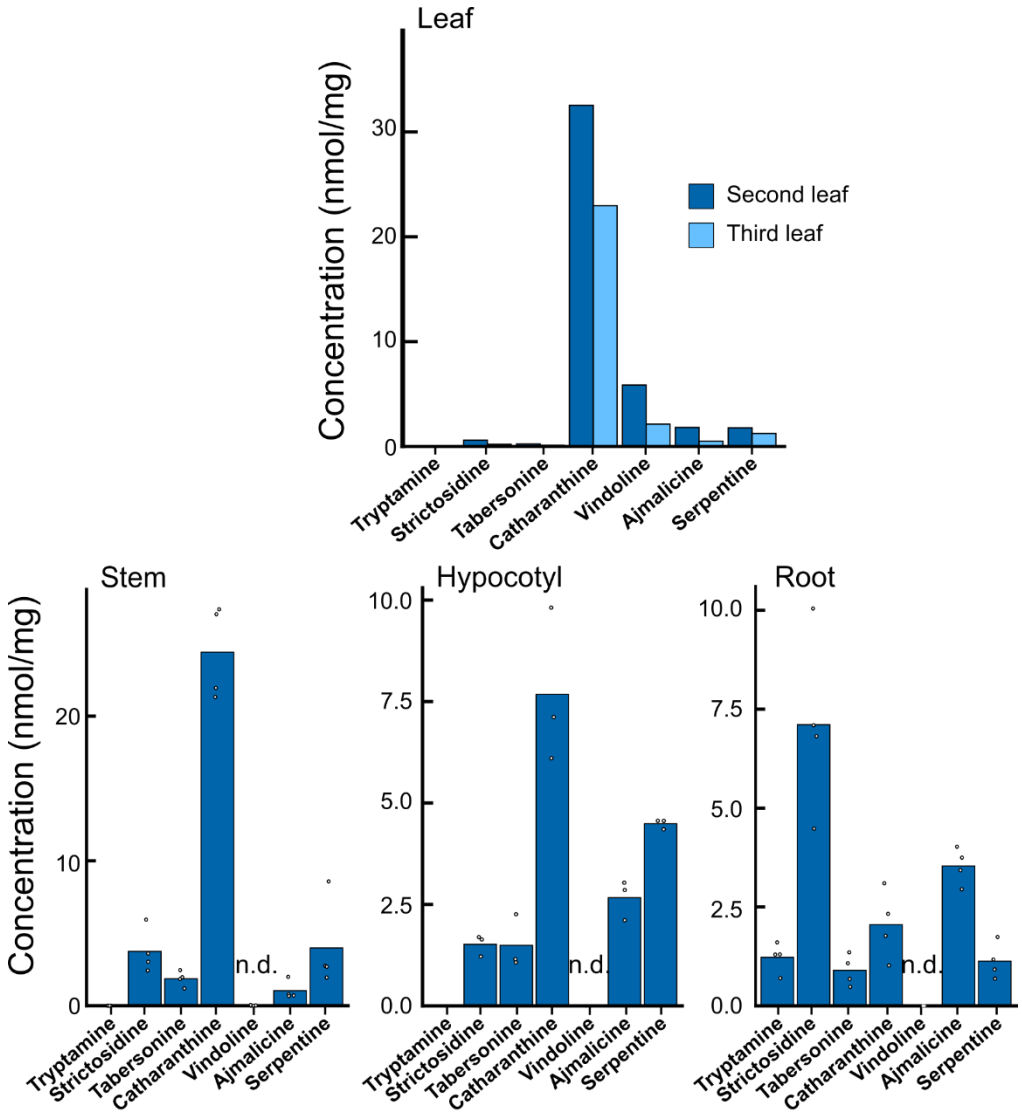

Fig. S15 Changes in embryo and endosperm iridoid content during seed imbibition and germination.

Bar graphs show changes in the content [nmol/10 embryos (above) or endosperms (below)] of each iridoid compound (n = 5). Each point represents an extract sample from 10 embryos or endosperms. N ≥ 5..

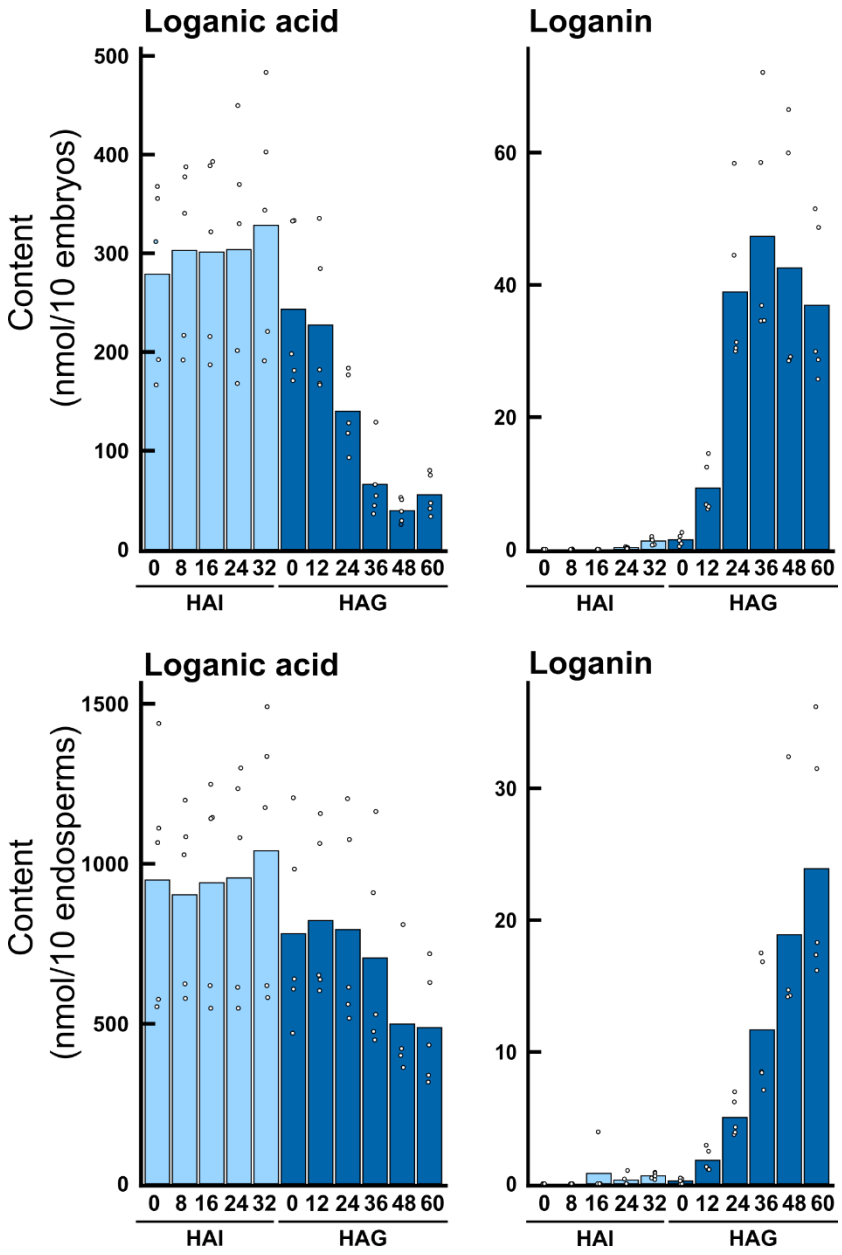

Fig. S16 MIA content changes in embryos dissected from seeds germinated under light.

Bar graphs show changes in MIA content of embryos from seeds that were allowed to imbibe in the dark and grown under light after 0 HAG. Each point represents an extract sample from 10 embryos. N ≥ 5..

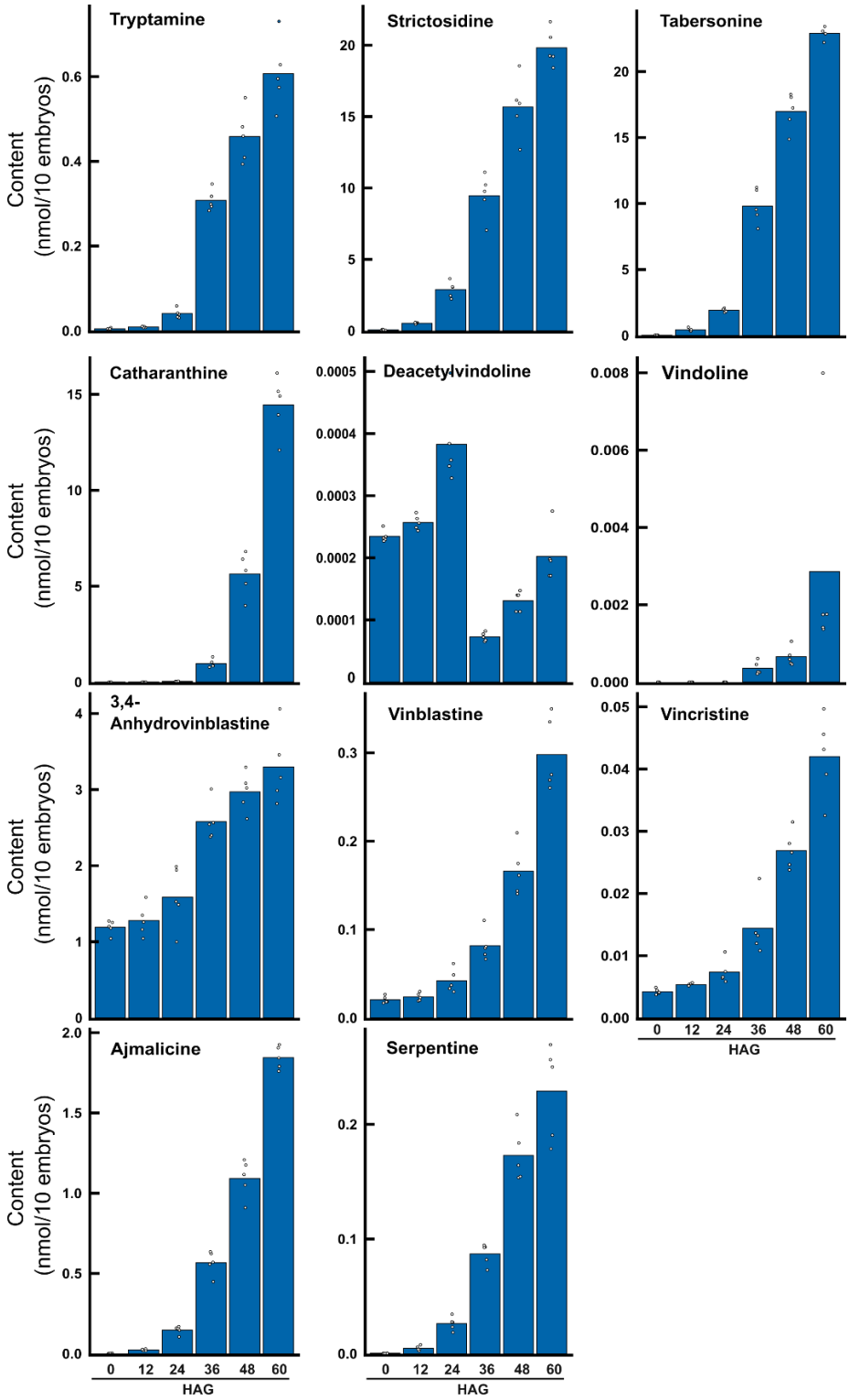

Fig. S17 Changes in endosperm MIA content during seed imbibition and germination.

Bar graphs show changes in MIA content in extracts from 10 embryos from germinating seeds (± standard error [SE]; n ≥ 5) for (**a**) all MIAs and (**b**) individual MIAs. Each point represents an extract sample from 10 endosperm. N ≥ 5.

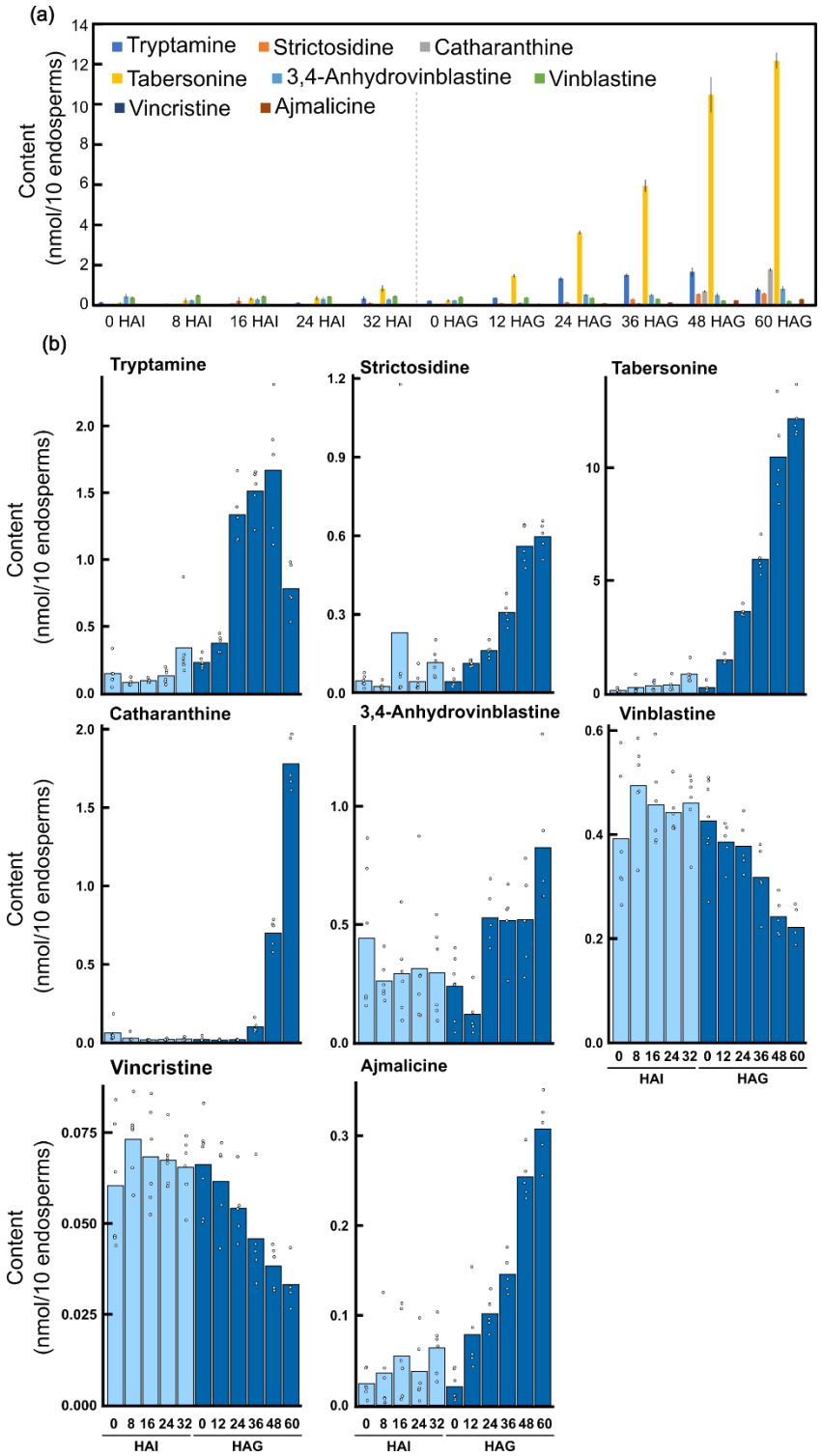

Fig. S18 Expression patterns of MIA biosynthetic enzyme genes in embryos from imbibing and germinating seeds

Bar graphs show average expression levels of MIA enzyme genes identified in embryos. Each RNA sample was extracted from 50 embryos and three biological replicates were conducted. Each plot represents one sample. TPM, transcripts per million. Enzyme gene abbreviations are provided in Fig. **1.**

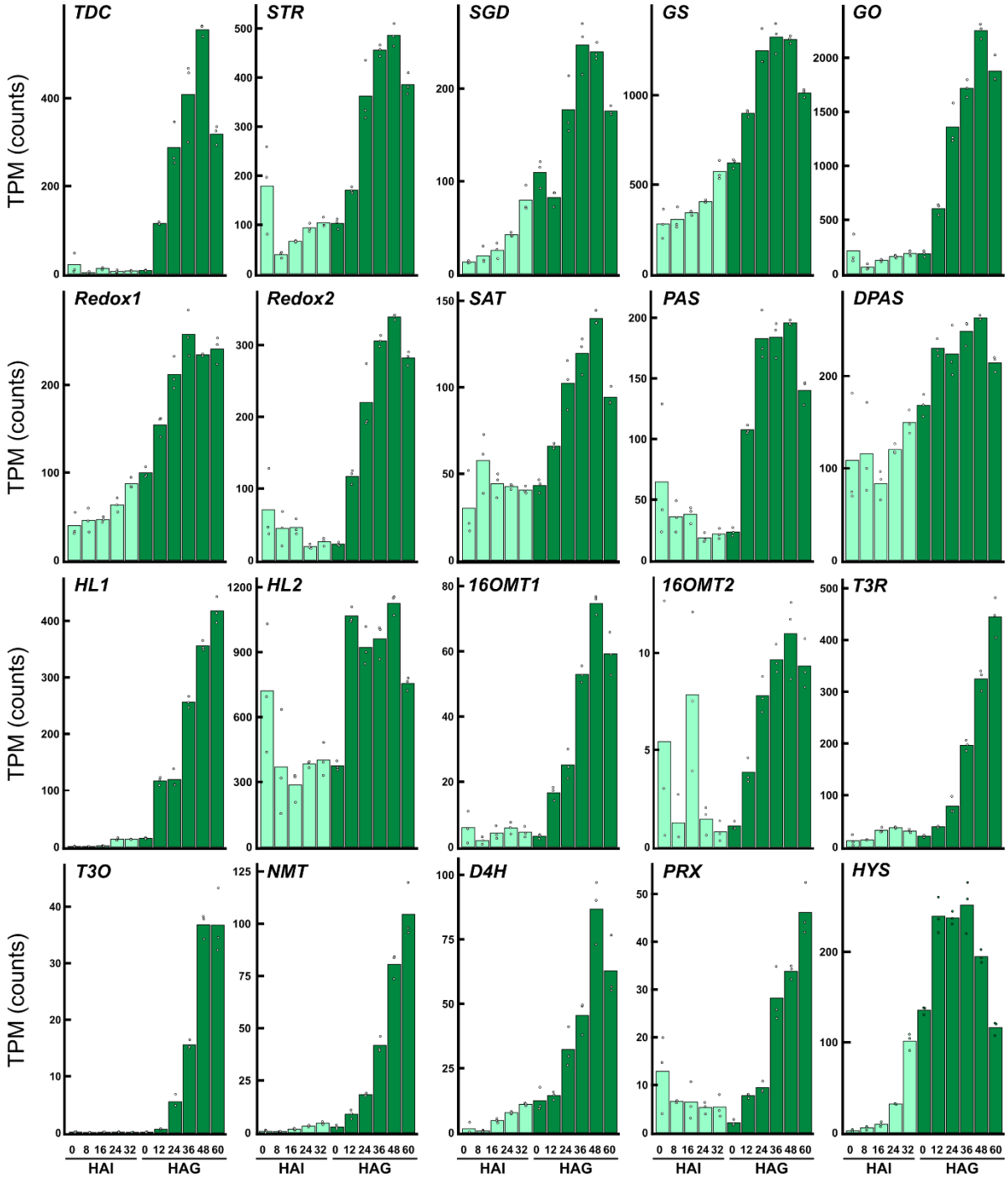

Fig. S19 Expression patterns of iridoid biosynthetic enzyme and related transcription factor genes in embryos of imbibing and germinating seeds.

Bar graphs show average expression levels of (**a**) identified iridoid biosynthetic enzyme genes and (**b**) related transcription factor genes in embryos. Each RNA sample was extracted from 50 embryos and three biological replicates were conducted. Each plot represents one sample. TPM, transcripts per million. Enzyme gene abbreviations are provided in Fig. **1**.

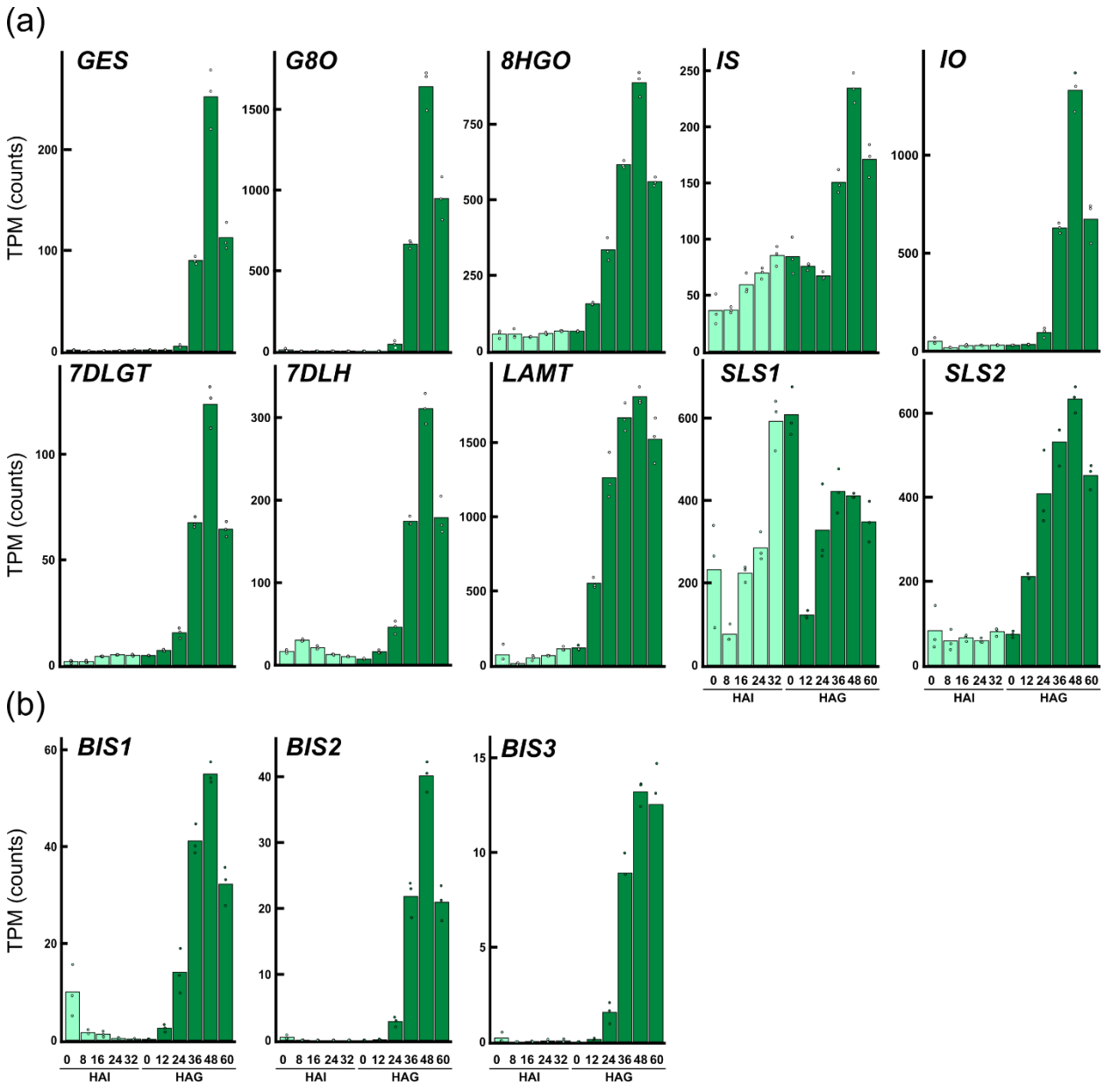

Fig. S20 Expression patterns of transcription factors related to MIA biosynthesis in embryos of imbibing and germinating seeds.

Bar graphs show average expression levels of identified transcription factors related to MIA biosynthesis in embryos. Each RNA sample was extracted from 50 embryos and three biological replicates were conducted. Each plot represents one sample. TPM, transcripts per million.

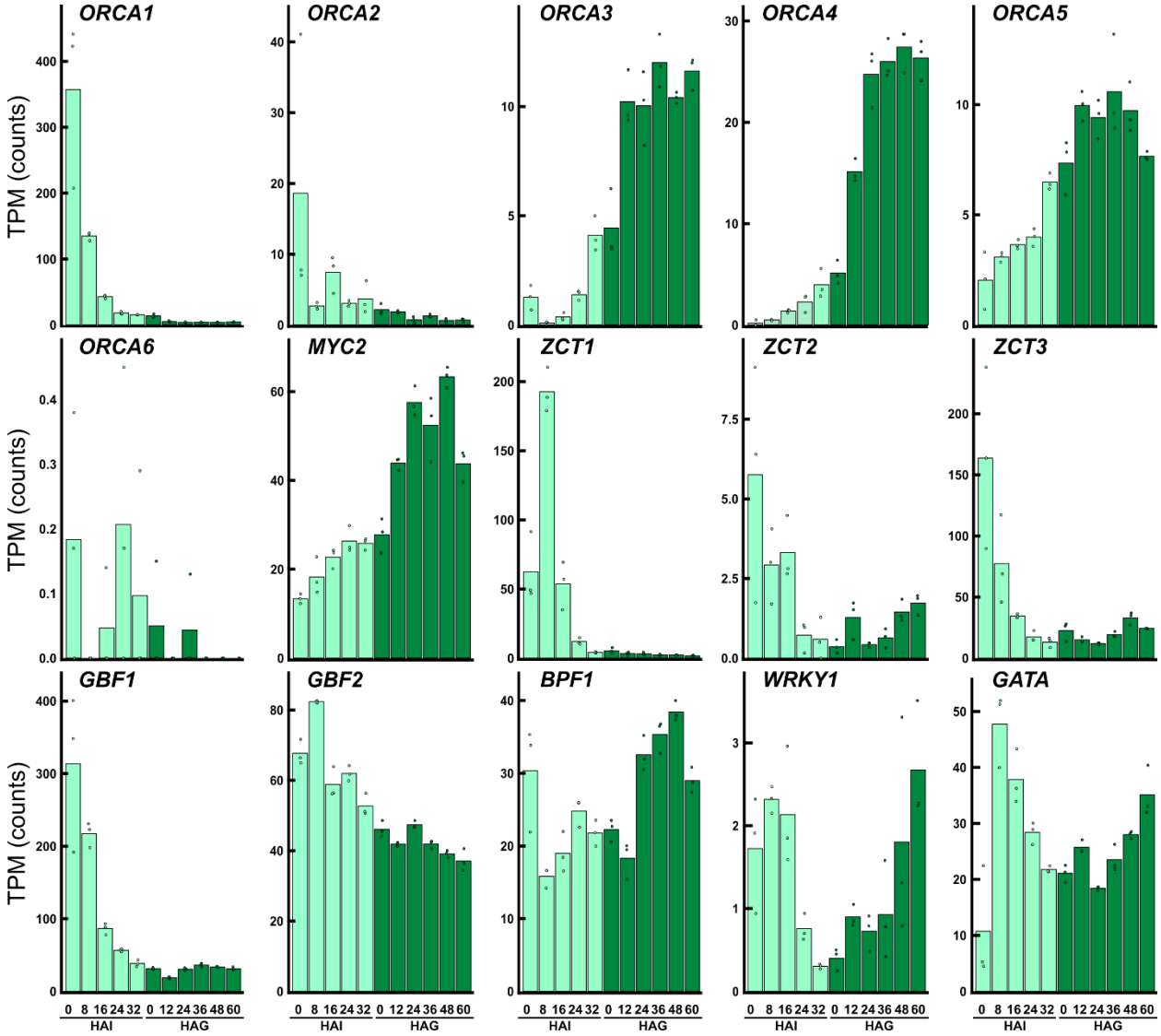

Fig. S21 Localization of compounds annotated as loganic acid, loganin or secologanin. Compounds with *m/z* = 415.1991, 429.1157, or 427.1001 were localized through IMS analysis of seeds, and annotated as loganic acid ([M+K]+), loganin ([M+K]+), and secologanin ([M+K]+), respectively. Scale bars are 1.0 mm.

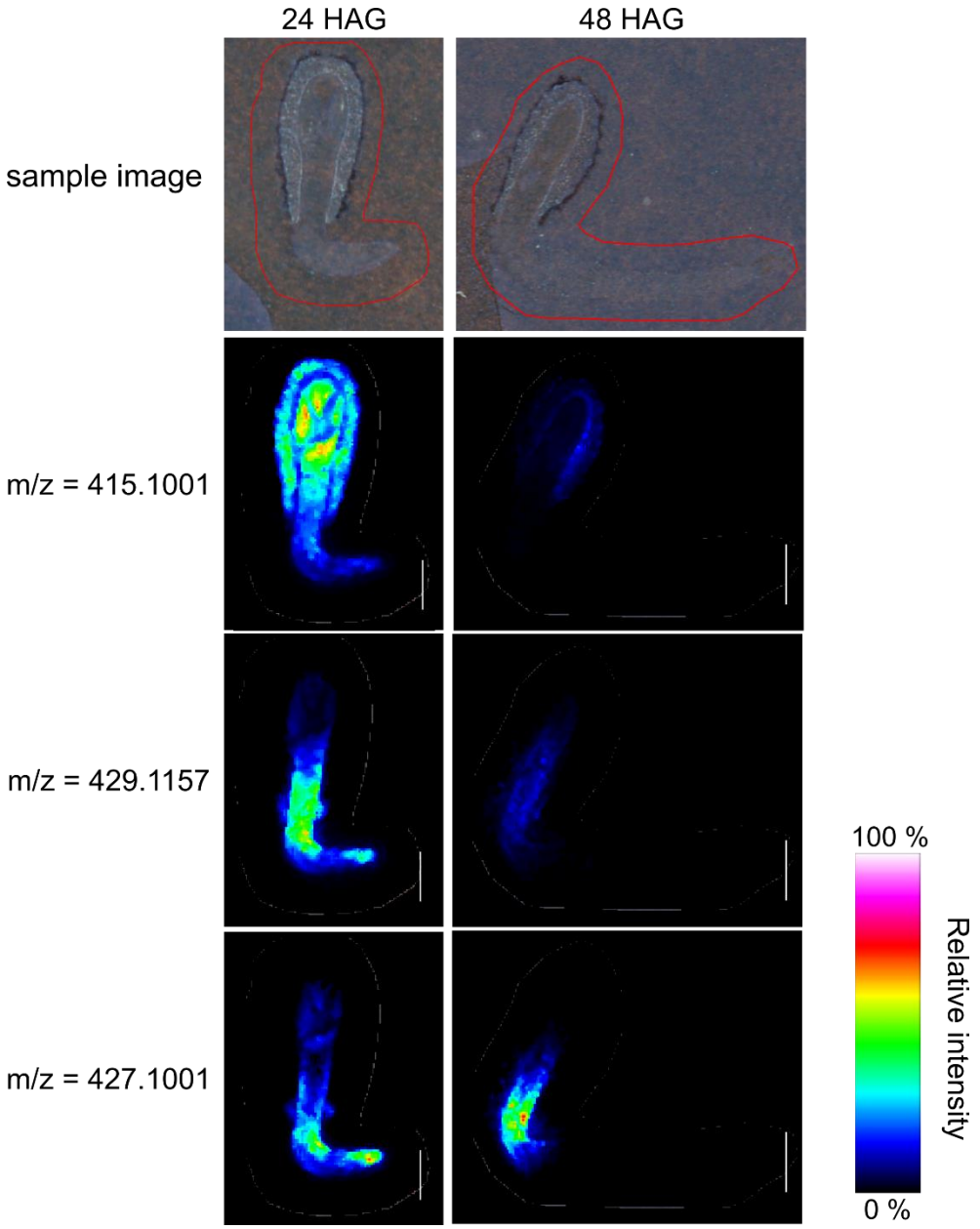

Table S1 Analytical conditions for liquid chromatography–tandem mass spectrometry (LC-MS/MS).

Analyte	RT (min)	MRM (*m/z*)	CID voltage (V)		
			Q1	CE	Q3
Tryptamine	0.845	161.1078 > 144.05*	−17	−13	−29
		161.1078 > 115.05	−17	−35	−30
Strictosidine	3.086	531.2342 > 514.15*	−28	−22	−26
		531.2342 > 144.05	−28	−37	−26
Catharanthine	3.700	337.1916 > 173.05*	−18	−16	−30
		337.1916 > 93.05	−18	−29	−19
Tabersonine	4.072	337.1916 > 173.05*	−18	−22	−15
		337.1916 > 228.15	−17	−22	−27
Diacetylvindoline	3.389	415.2333 > 188.1*	−22	−36	−19
		415.2333 > 355.15	−12	−25	−26
Vindoline	4.547	457.2338 > 188.05*	−22	−38	−22
		457.2338 > 397.1	−24	−22	−19
3,4-Anhydrovinblastine	5.202	397.2 > 367.15*	−20	−18	−10
		397.2 > 262.55	−19	−22	−30
		793.4 > 337	−24	−39	−17
Vinblastine	4.490	406.2179 > 271.6*	−20	−26	−25
		406.2179 > 376.2	−20	−20	−19
		811.428 > 224.3	−26	−39	−24
Vincristine	4.074	413.2076 > 362.1*	−21	−22	−27
		413.2076 > 353.2	−22	−25	−26
Ajmalicine	3.523	353.1865 > 144.05*	−18	−27	−30
		353.1865 > 115	−29	−55	−30
Serpentine	3.957	349.1552 > 263.05*	−18	−31	−30
		349.1552 > 317.1	−18	−25	−21
Ajmaline	2.315	327.2072 > 144.05*	−16	−38	−29
		327.2072 > 158.1	−17	−40	−27
Loganic acid	1.310	399.1267 > 219.0*	−21	−24	−15
		399.1267 > 236.95	−21	−22	−25
Loganin	2.610	413.1422 > 219.1*	−22	−25	−15

		413.1422 > 251.05	−22	−23	−12
Secologanin	3.275	411.1267 > 249.05*	−21	−23	−17
		411.1267 > 255.05	−21	−22	−12

CID, collision-induced dissociation; MRM, multiple reaction monitoring; RT, retention time.

* MRM transition used for quantification.

Table S2 2 Normalized peak intensity of compounds with *m/z* = 337.19, 349.15, 353.18, or 355.20 detected through non-targeted LC-MS/MS analysis in *C. roseus* embryos

RT (min)	*m/z*	Annotation	0 HAI	8 HAI	16 HAI	24 HAI	32 HAI	0 HAG	12 HAG	24 HAG	36 HAG	48 HAG	60 HAG
4.797	337.190	Catharanthine	0.0462	0.0411	0.0322	0.0437	0.0486	0.0476	0.1762	1.2583	12.2918	84.0168	184.4920
4.367	337.190		0.1151	0.1694	0.1918	0.1566	0.2736	0.1279	0.7371	2.4923	5.1269	14.6297	30.0579
5.236	337.190	Tabersonine	0.7250	0.9254	1.4363	1.5640	2.4202	0.6965	20.0522	78.8896	169.3009	352.9375	570.9835
2.053	337.191		0.0026	0.0009	0.0018	0.0019	0.0016	0.0019	0.0028	0.0048	0.0453	0.3518	1.0987
2.493	337.191		0.0061	0.0019	0.0023	0.0027	0.0031	0.0036	0.0079	0.1241	1.4593	9.8345	27.3192
3.03	337.191		0.0087	0.0026	0.0029	0.0040	0.0043	0.0050	0.0088	0.1245	1.2882	8.2625	23.4214
5.605	349.154		0.0036	0.0021	0.0029	0.0049	0.0039	0.0032	0.0126	0.0396	0.0969	0.2106	0.3112
5.138	349.155	Serpentine	0.0376	0.0442	0.0220	0.0207	0.0524	0.0227	0.3146	1.7994	8.8522	20.1631	37.5486
5.335	349.155	Alstonine	0.0045	0.0038	0.0043	0.0040	0.0048	0.0058	0.0422	0.1006	0.1887	0.3416	0.5846
6.765	349.155		0.0036	0.0018	0.0028	0.0031	0.0020	0.0035	0.0060	0.0123	0.0173	0.0394	0.0926
4.606	353.185	Tetrahydroalstonine	0.0359	0.0755	0.0792	0.1230	0.1535	0.0527	0.9136	5.3000	14.1582	33.0706	48.9915
3.016	353.185		0.0231	0.0262	0.0301	0.0273	0.0479	0.0326	0.1017	0.5445	2.1854	7.7302	15.9894
2.126	353.185		0.0023	0.0017	0.0022	0.0020	0.0019	0.0023	0.0035	0.0478	0.3851	2.0400	5.2247
4.75	353.185	Ajmalicine	1.1669	4.7508	3.6866	4.8404	4.9287	0.9864	3.7043	21.0915	35.6052	64.0341	67.3972
3.129	353.185		0.0178	0.0164	0.0155	0.0156	0.0392	0.0217	0.0971	0.6368	1.5655	2.9796	5.9957
5.178	353.186		0.0276	0.0363	0.0325	0.0393	0.0468	0.0281	0.1370	0.4554	0.8647	1.5963	2.3720
5.03	355.201		0.0026	0.0028	0.0022	0.0026	0.0027	0.0020	0.0073	0.0355	0.3392	4.7304	26.0371
3.445	355.201	Corynanthine	0.0135	0.0337	0.0219	0.0548	0.1776	0.0736	0.7921	1.5169	2.8942	6.0186	7.4030
5.73	355.201		0.0054	0.0121	0.0145	0.0225	0.0188	0.0086	0.0297	0.0312	0.0463	0.0508	0.1063
4.081	355.210		0.0019	0.0039	0.0062	0.0074	0.0127	0.0093	0.0880	0.4207	1.2150	3.0985	4.2854

3.14	355.210		0.0108	0.0109	0.0113	0.0103	0.0315	0.0235	0.1759	1.2514	2.5094	3.2981	4.9053

RT, retention time; HAG, hours after germination; HAI, hours after imbibition.

Reference

Bolger AM., Lohse M & Usadel B. 2014. Trimmomatic: a flexible trimmer for Illumina sequence data. *Bioinformatics*, 30**,** 2114-20.

Dawson C. 2022. ggprism: A 'ggplot2' Extension Inspired by 'GraphPad Prism'. R package version 1.0.4. https://cran.r-project.org/package=ggprism doi: 10.5281/zenodo.4556067Hmisc: Harrell Miscellaneous.

Dobin A, Davis CA., Schlesinger F, Drenkow J, Zaleski C, Jha S, Batut P, Chaisson M & Gingeras TR. 2013. STAR: ultrafast universal RNA-seq aligner. *Bioinformatics*, 29**,** 15-21.

Gentleman R, Carey V, Huber W, Hahne F. 2023. genefilter: genefilter: methods for filtering genes from high-throughput experiments. doi:10.18129/B9.bioc.genefilter, R package version 1.84.0, https://bioconductor.org/packages/genefilter.genefilter: genefilter: methods for filtering genes from high-throughput experiments.

Li B. & Dewey CN. 2011 RSEM: accurate transcript quantification from RNA-Seq data with or without a reference genome. *BMC Bioinformatics*, 12**,** 323.

Tsugawa H, Cajka T, Kind T, Ma Y, Higgins B, Ikeda K, Kanazawa M, Vandergheynst J, Fiehn O & Arita M. 2015. MS-DIAL: data-independent MS/MS deconvolution for comprehensive metabolome analysis. *Nature Methods*, 12**,** 523-526.

Uzaki M., Yamamoto K, Murakami A, Fuji Y, Ohnishi M, Ishizaki K, Fukaki H, Hirai MY & Mimura T. 2022. Differential regulation of fluorescent alkaloid metabolism between idioblast and lacticifer cells during leaf development in Catharanthus roseus seedlings. *J Plant Res*, 135**,** 473-483.

Warnes GR, Bolker B, Bonebakker L, Gentleman R, Huber W, Liaw A, Lumley T, Maechler M, Magnusson A, Moeller S, et al. 2020. gplots: Various R Programming Tools for Plotting Data.

Wickham H. 2016. ggplot2: Elegant Graphics for Data Analysis. Springer-Verlag New York. ISBN 978-3-319-24277-4, https://ggplot2.tidyverse.org.

Wickham H, Averick M, Bryan , Chang W, McGowan L, François R, Grolemund G, Hayes A, Henry L, Hester J, et al. Welcome to the Tidyverse. *Journal of Open Source Software,* 4**,** 1686.

Wickham H. 2023. stringr: Simple, Consistent Wrappers for Common String Operations. R package version 1.5.1, https://github.com/tidyverse/stringr, https://stringr.tidyverse.org.

Wickham H, François R, Henry L, Müller K, Vaughan D 2023. dplyr: A Grammar of Data Manipulation. R package version 1.1.4, https://github.com/tidyverse/dplyr.